AN OPTICAL MODEL OF THE FIX-FOCUS SCHEFFLER REFLECTOR

De Wet van Rooyen*, Anna Heimsath, Peter Nitz, Werner Platzer

Fraunhofer Institute for Solar Energy Systems (ISE), Heidenhofstr. 2, 79110, Freiburg, Germany

* +49 (0) 0761/4588-5971, Fax: +49 (0) 761/4588-5981, E-mail: de.wet.van.rooyen@ise.fraunhofer.de

1. Introduction

The Scheffler Reflector (SR) is a fix-focus parabolic type solar concentrator applied to produce heat for industrial processes (Jayasimha 2006) and potentially for the generation of electricity as well. An optical model has been developed to study the characteristics of the Scheffler Reflector with a ray tracing algorithm.

1.1 Development History

The original design of the SR was conceptualised by Wolfgang Scheffler to enable construction in rural workshops of developing countries. The energy available at the focal point was intended to be used for cooking purposes. The improvement this development brought with it was the fact that cooking with the power of the sun could take place indoors (Oelher and Scheffler 1994). The reflectors are positioned outside (on the northern side of the house in the northern hemisphere) and reflect the sun's energy to holes in the wall (focus is spot fixed in space) through which the concentrated radiation reaches and heats cooking vessels.

Figure 1: Scheffler Reflector steam system at a Mount Abu hospital in Rajasthan, India.[Source: Heike Hoedt]

In the late 1990's further development of the application saw the construction of the first SR solar steam kitchens in India. The receivers of the SRs were connected by a header pipe, enabling the production of saturated solar steam at an operating pressure of 8 to 12 bar (corresponding to temperatures up to 190 °C) (Pilz 2006; GTZ 1997). The SR systems thus have been delivering solar process heat (SPH) in the medium temperature range since 1997.

Wolfgang Scheffler and Heike Hoedt have been accompanying and driving development of this technology for many years and have supported this work with advice and sharing of their experience.

1.2 Components

To understand how the SR tracks the sun throughout the day, changes its shape throughout the year and how it is installed, knowledge about the three assembly groups (stand, rotating support, reflector) is required. In the following figure the colour coded components groups can be seen. The yellow axis of (daily) rotation is actually welded to the purple rotating support.

The stand has to carry the whole structure and defines the orientation (north-south), inclination (according to the latitude of the installation site, see Figure 7) and height of the axis of daily rotation.

The rotating support is installed on the stand and its main function is to support the dish as it turns about the axis of daily rotation.

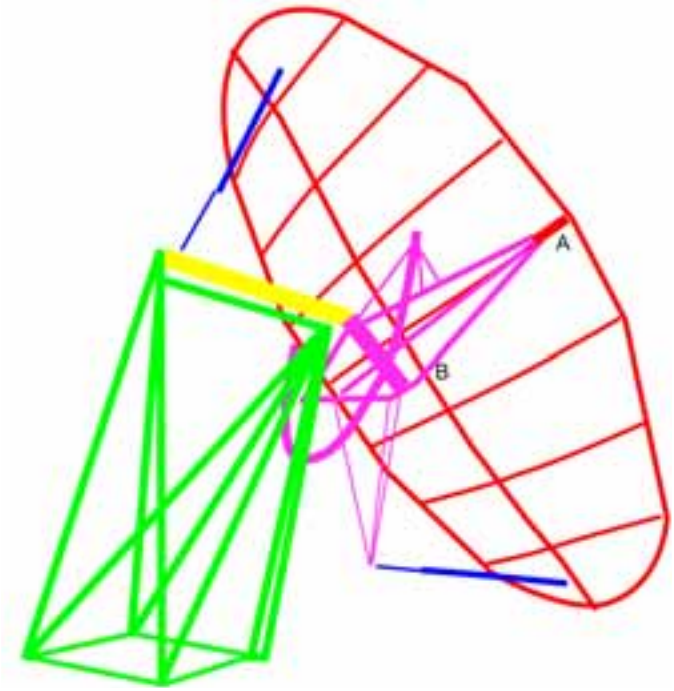

Figure 2: Components of Scheffler Reflector: Stand (Green), Daily Rotation Axis (Yellow), Rotating Support (Pink), Dish {Elliptic Frame, Centerbar and Crossbars} (Red), Seasoal Adjustment linear actuators (Blue)

The reflector is mounted in the rotating support at three nonlinear points (points "A" at the sides and "B" on the center bar). Furthermore two telescope bars connect the ends of the center bar to the rotating support. They serve in adjusting the reflector according to the declination of the sun. The crossbars, center bar and elliptical frame are welded together to form the carrying structure of the reflective material. These components are constructed as two-dimensional curvatures for a specific declination of the sun (equinox). These curves all lie in a rotational paraboloid as can be seen in Figure 3. The form of the reflector at equinox is thus a section from the side of a rotational paraboloid.

Figure 3: The paraboloid with crossbars, center bar and the elliptical frame as curves on the paraboloid surface.

The aperture area Ap_0 of the dish is defined by the area enclosed by the elliptical frame at equinox. This area is used as reference when expressing the optical efficiency based on direct normal irradiation (DNI).

For industrial applications glass mirror tiles are used to cover the surface of the SR. As the SR was originally designed to make use of locally available material, normal bathroom mirror tiles were cut to size and given one to two coatings of acrylic paint at the back and cut edges to prevent corrosion of the specular coating in ambient conditions. The mirror tiles are then fixed to so-called "long bars"

Glass mirror tiles, if prepared correctly before installation, may last more than fifteen years. Should one break, it is easy to replace. Due to gaps between the mirror tiles not the whole surface of the dish is reflecting.

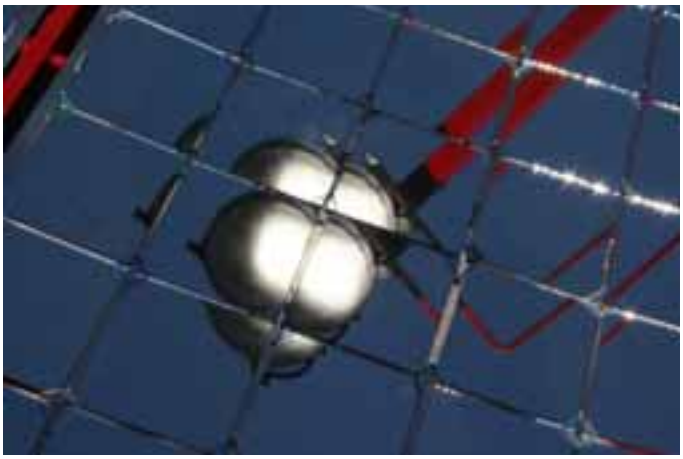

Figure 4: The focal point of a 2.7 m² Scheffler Reflector solar cooker is seen reflected in the mirror tile segments of its primary reflector.[Source: Denis-Luc Ardiet]

The receivers used in most steam systems resemble flasks. They are made of normal steel and the produced steam is fed into a header pipe. The inlet of the receiver is also in the header pipe, but below the water surface, thus making sure that the receiver is always filled with water during operation. Receivers of this type are generally produced with a diameter of forty centimetres.

Figure 5: An example of a round flask shaped receiver used with Scheffler Reflector process heat steam systems.[Source: De Wet van Rooyen]

2. Functioning Principles

The fix focus attribute of the collector is achieved by adjusting the three dimensional curvature of the reflector in dependence of the solar declination (adjusted shape of reflector referred to as “reflector declination” δ_r) and tracking the sun throughout the day by rotation of the SR about a rotation axis (yellow in Figure 2) which is aligned parallel to the earth's axis of rotation. In Figure 6 the axis of daily rotation is depicted with a dotted “x-axis”. It can also be seen that the focal length of the paraboloid at equinox (F0) is shorter than the focal length of the parboloid at the winter solstice (Fw) and larger than the focal length of the paraboloid at the summer solstice (Fs).

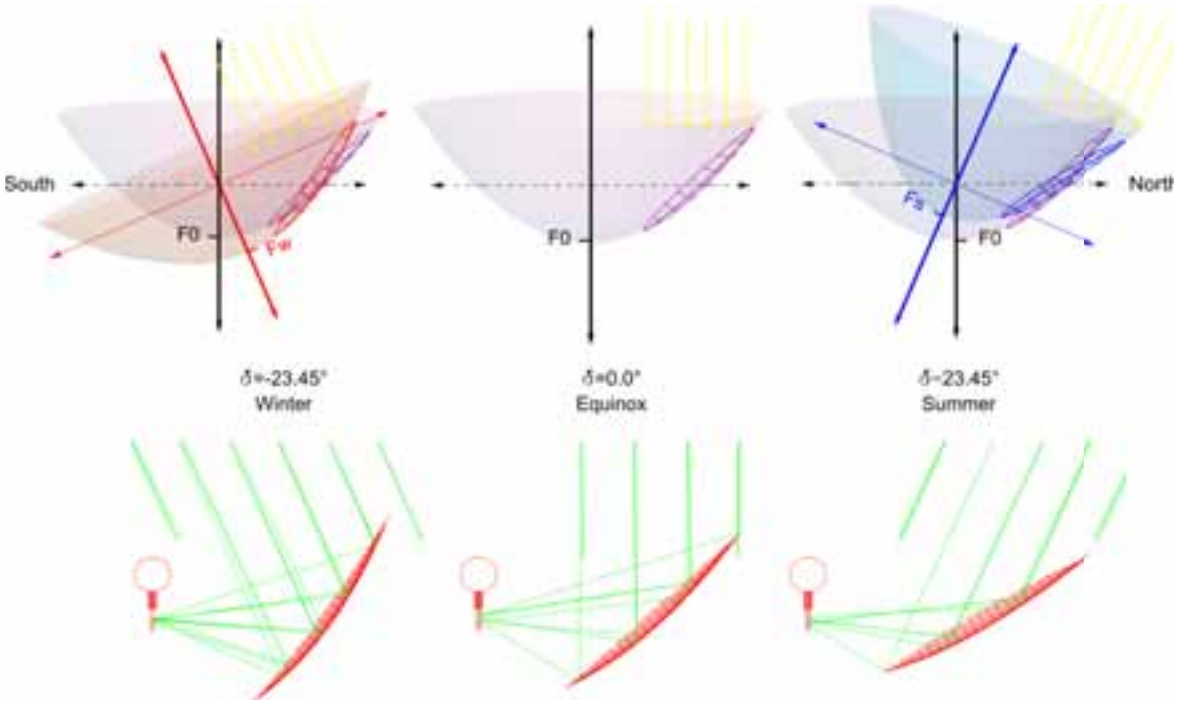

Figure 6: Sections of paraboloids for three different seasonal declinations (Winter solstice, equinox and summer solstice) at solar noon..

This axis is always installed at an inclination equal to the latitude at which the device is located (see Figure 7).

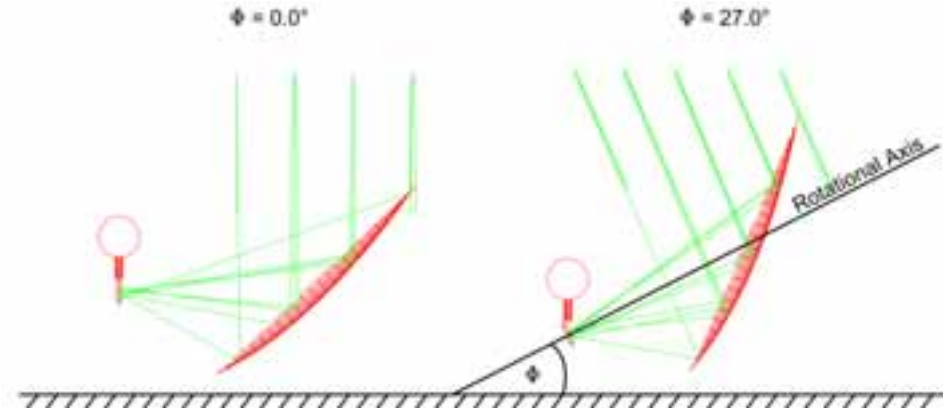

Figure 7: Two reflectors at equinox and solar noon at different latitudes. The inclination of the daily rotation axis corresponds to the latitude at the site. Furthermore the axis of rotation is aligned with the true north-south line.

For a perfectly tracked and adjusted system the direct beam incidence angle on the aperture of the SR (θ in the following) is given in dependence of only the declination δ_s of the sun.

$$\theta(\delta_s) = \tan^{-1}(0.93986) + \frac{\delta_s}{2} \qquad \text{(eq. 1)}$$

The effective aperture of the SR thus stays constant throughout the day but changes throughout the year as can be seen in the following figure.

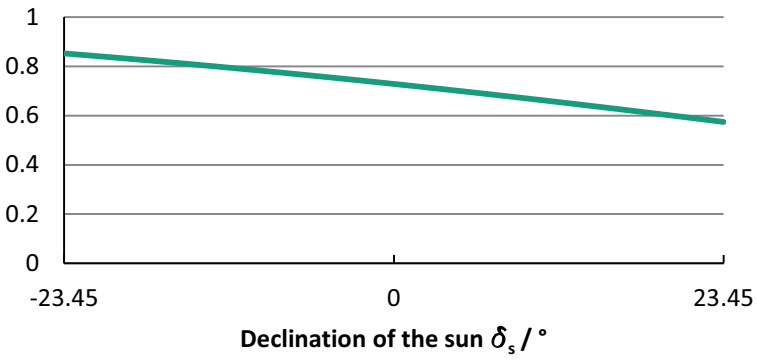

$$\cos\left(\tan^{-1}(0.93986) + \frac{\delta_S}{2}\right)$$

Figure 8: The cosine factor of the incidence angle of the direct beam radiation on the aperture of Scheffler Reflector.

3. Optical Modelling

A theoretical geometrical model was developed to enable a full theoretical analysis of the optical characteristics and behavior of the Scheffler Reflectors (SR). The theoretical model for the site and time dependent geometry of the SR was than implemented into the Fraunhofer ISE simulation environment Raytrace3D.

1.3 Raytrace3D – Ray tracing algorithm

Raytrace3D is a monte-carlo forward ray tracer, describing the characteristics of rays as they are influenced by the defined optical characteristics (absorptance, transmittance and reflectance) of geometries with which they are incident and eventually the spatial intensity distribution of the incident rays on the receiver. A ray which is incident with a geometric object is thus treated according to the defined characteristics of the object following the laws of refraction and reflection according to geometrical optics.

The light source in Raytrace3D incorporates the sunshape distribution either by a defined Gaussian standard deviation or by measured values or other representations of a sunshape distribution function as input from a "sunshape file".

A specular surface error (σ_{surface}) and reflectance value (ρ) is defined for all reflecting surfaces. For absorbing surfaces (such as representing the receiver in the model) an absorptance value is defined. Furthermore the absorber plane is divided into a specified number of bins in order to register a ray hit and display the spatial intensity distribution of the radiation on the absorber surface. Transparent media can also be modelled requiring a transmittance value. The so-called "absorber file" supplies the spatial intensity distribution on a defined receiver area and allows further analysis of the ray tracing simulation results.

Raytrace3D was developed for resource efficient simulations of linear Fresnel collectors (Mertins 2009) and later enhanced for parabolic trough collectors, solar dishes and power tower systems (Branke 2010).

1.4 The Scheffler Reflector model

An algorithm was developed to generate the geometries (rectangular mirror tile segments tangential to paraboloidal surface with required orientation and spacing) representing the reflective surface of the SR dish. Table 1 gives a list of geometrical input parameters for the SR model used for the results displayed in section 4

Table 1: Input Parameters for Scheffler Reflector model

Parameter	Description	Default
F0	Focal length of paraboloid at equinox (Size of reflector)	2,02638 m (Ap0=16,17221 m)
Mh	Mirror tile height	0,23 m
Mw	Mirror tile width	0,17 m
D	Distance between mirror tiles	0,002 m
latitude	Latitude of site	30.0°
eps_latitude	Rotation inclination axis error	0.0°
eps_NS	Deviation of rotation axis orientation from true north-south	0.0°
omega_r	Hour angle of reflector	-
delta_r	Declination of reflector	-
abs_r	Absorber radius	0,2 m
abs_s	Deviation of Absorber position along axis of rotation	0.0 m

With these parameters the size, position, orientation (relative to the sun) and shape (declination) of the reflector is defined. Furthermore the size and position of the absorber plane can be defined relative to the ideal focal point. Figures 1,2 and 7 depict geometries as generated by the SR Model.

Figure 9: Scheffler Reflector with different mirror tile geometries

Certain assumptions have to be made about the shape accuracy of the SR. Hafner (1999) stated the shape error (σ_{shape}) of the SR is an average of 1.5° (0,026 rad). Together with the assumed spectral surface error (σ_{surface}) of planar glass mirrors, this results in the total error (σ_{total}) if the errors are assumed to have an isotropic Gaussian distribution.

$$\sigma_{\text{total}} = \sqrt{\sigma_{\text{surface}}^2 + \sigma_{\text{shape}}^2} \qquad \text{(eq. 2)}$$

For the following simulations a total optical error (combined surface and shape) with a standard deviation of 0.026 rad is assumed as the specular surface error is of planar mirrors is negligible compared to the shape error. The sunshape distribution is assumed to have a circumsolar ratio (CSR) of 17 percent(Neumann et al. 2002). Unless stated otherwise the mirror tile geometry given in Table 1 is used.

The reflectance of the glass mirror tiles is assumed to be 0.92. The absorber surface will be represented by a planar disc with a radius “r” in the following simulations. The absorptance of the receiver is taken as 0.9.

4. Results

The optical characteristics of the SR can be described by its receiver intercept factor, optical efficiency and acceptance angle.

The receiver intercept factor $\gamma(\mathrm{r})$ is defined as the fraction of rays which are incident on the receiver aperture (disc with radius “r”) relative to the number of rays incident on the absorber plane.

$$\gamma(\mathrm{r}) = \frac{N_{\text{rays}}^{\text{Receiver}_{\text{Ap(r)}}}}{N_{\text{rays}}^{\text{Absorber Plane}}} \qquad \text{(eq. 3)}$$

The extension of the focal spot in the focal plane is defined to a large extent by the geometry of the planar

mirror tiles used in the model for the primary reflective surface. The receiver intercept factor ($\gamma(r)$) can thus be adjusted by choice of absorber aperture radius.

Width and height of the mirror tiles have been varied to assess their influence on the optical performance. In Figure 10 it can be seen that the choice in mirror tile geometry determines the receiver intercept factor for a given receiver aperture radius.

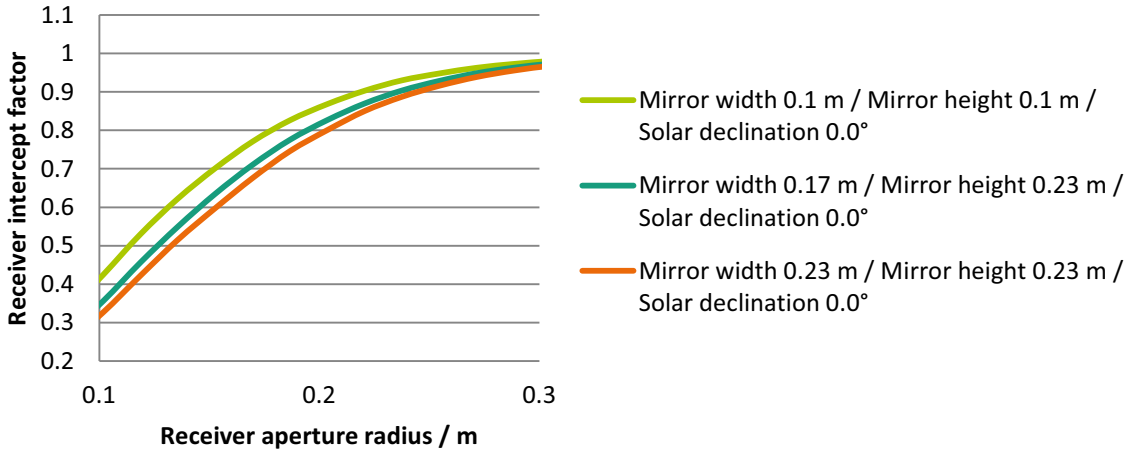

Figure 10: Receiver intercept factor for different mirror tile geometries at equinox over a receiver aperture radius range of 0.1 m to 0.3 m. Mirror width (Mw), mirror height (Mh) and receiver aperture radius in meters.

Furthermore the intensity distribution of the focused solar radiation on the absorber plane changes throughout the year. For a chosen mirror tile geometry with width 0.17 m and height 0.23 m three curves in Figure 11 depict the way in which the receiver intercept consequently changes throughout the year. This effect also influences the optical efficiency of the SR as can be seen in Figure 13.

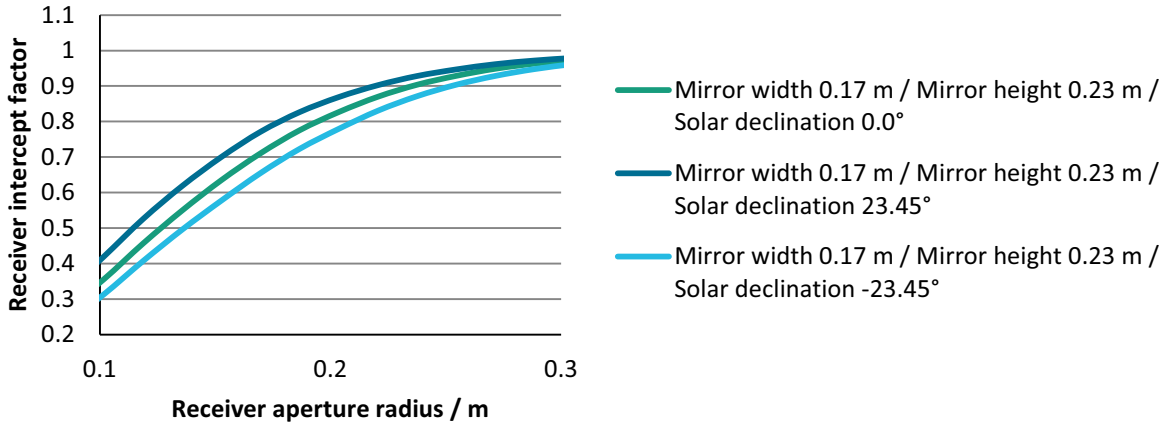

Figure 11: Receiver intercept factor for different times of the year (equinox, summer solstice and winter solstice) for a specific mirror tile geometry. Mirror width (Mw), mirror height (Mh) and receiver aperture radius in meters.

The optical efficiency η_{opt} takes further factors into account such as the reflectivity of the primary mirror, the cosine factor (incidence angle of I_{beam} on the primary reflector), the packing ratio ρ_{packing} and the absorbtivity of the receiver (α).

$$\eta_{\text{opt}} = \frac{\text{Absorbed radiation}}{\text{DNI} \times \text{Ap}_0} \qquad \text{(eq. 4)}$$

The packing ratio is retrieved by projecting each mirror tile onto the plane of elliptical frame at equinox and dividing the sum of these projected areas by the aperture. This value varies in dependence of the chosen mirror tile geometry, gap size between the mirror tiles and packing procedure followed. In Figure 12 the packing ratios achieved with different mirror tile geometries is represented. In all cases the starting position

from which the packing begins is the same. The packing ratio is an expression of how large the fraction of reflective surface of the SR aperture is. A high packing ratio is an indication that the available surface area is used well.

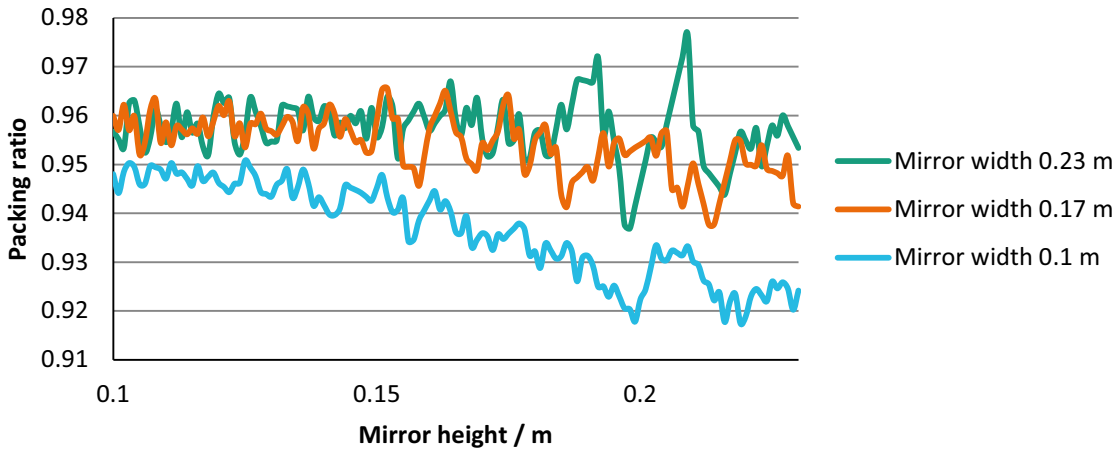

Figure 12: Packing ratio variation for different mirror tile geometries, plotted against height Mh of the the mirror tiles.

From Figure 12 it is clear that a smaller mirror tile leads to a lower packing ratio. A higher packing ratio can be achieved if the mirror height is smaller than the mirror width. Within a range of 0.1 m and 0.23 m the maximum packing ratio (0.97907) was achieved with mirror tiles with a width of 0.217 m and a height of 0.122 m.

The optical efficiency was generated in dependence of the solar declination for a perfectly seasonally adjusted SR with two sets of parameters. The first set was based on the assumptions as described in section 1.4 and can be seen in Figure 13 as the lowest curve. Depicted again is the cosine factor of the beam radiation's incidence angle on the SR's aperture (see upper curve Figure 13). The orange curve depicts the optical efficiency of a SR with the newly optimized mirror tile geometry and a reduced shape error. It can be seen that the cosine factor as given in equation 1 influences the optical efficiency's trend throughout the year. From the graph it is also evident that the difference to the cosine value is higher in winter (solar declination = -23.45°) than in summer (solar declination = 23.45°). This can be ascribed to the higher receiver intercept factor in summer. The light blue curve in Figure 13 was generated by implementing the optimized mirror geometry, but assuming a shape error as described by Hafner (1999).

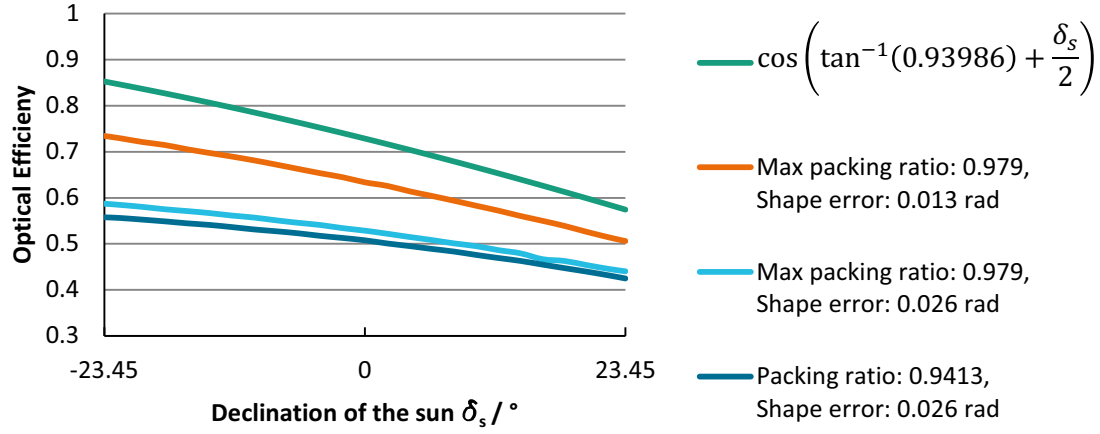

Figure 13: Optical efficiency improvement through choice of mirror tile geometry and lower shape error.

For stationary collector systems, the acceptance angle is defined as the angle within which all radiation incident on the aperture is reflected to the absorber (Duffie and Beckman 2006). The geometry and functioning principles of the Scheffler Reflector however does lead to a change in the intensity distribution within the absorber aperture for any misalignment of the reflector with the I_{bn} direction. The acceptance angles $\theta_{c,\omega}$ and $\theta_{c,\delta}$ are defined as the angles within which 90% of the radiation is incident on the absorber aperture for deviations between the solar and reflector declination and hour angle respectively.

At equinox the optical efficiency is reduced more with every degree the sun's declination becomes more positive compared to the deviation in the negative direction. This behavior can partly be ascribed to the increase of effective aperture of the SR if $\delta_r - \delta_s$ is positive. For a receiver aperture of 0.2 m the reduction in optical efficiency is portrayed in Figure 14 for a deviation of the solar declination at a reflector declination of -23.45° and 23.45°.

$\theta_{c,\delta}$ thus lies between 1.1° at the winter solstice and 1.4° at the summer solstice for a SR with parameters as defined in Table 1.

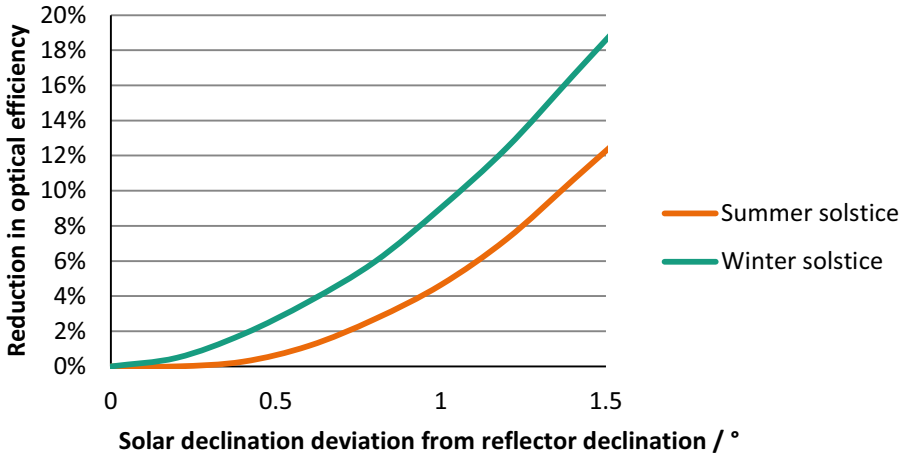

Figure 14: Reduction in optical efficiency due to the difference between solar and reflector declination at solstices.

To assess the influence of daily tracking accuracy, a deviation between solar hour angle and hour angle of the SR has been modeled. There seems to be no significant difference in the deterioration of optical efficiency with an hour angle tracking error throughout the year (See Figure 15). $\theta_{c,\omega}$ has an average value of 1.25° throughout the year.

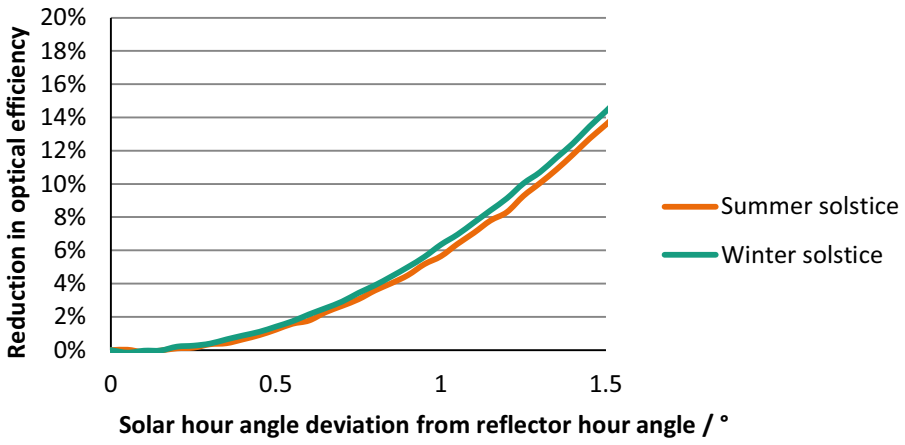

Figure 15: Reduction in optical efficiency due to the difference between solar and reflector hour angle at solstices.

5. Conclusion

The developed geometrical model for the ray tracing analysis is versatile and flexible allowing the study of numerous effects and circumstances influencing the optical efficiency of the Scheffler Reflector. Through variation of parameters improved, optimized configurations can be found for specific sizes of the Scheffler Reflector with respect to the optical efficiency as depicted in Figure 13.

The receiver intercept factor is dependent on the mirror tile geometry used for constructing the primary mirror surface. Furthermore the change in intercept throughout the year influences the optical efficiency seasonally.

The packing ratio also varies depending on the chosen mirror tile geometry. Whereas smaller mirror tiles might ensure a larger receiver intercept factor (for a specific absorber aperture radius), the induced relatively large total gap area between the mirror tiles reduces the packing ratio, thereby reducing the effective aperture.

With a deviation from the optimal orientation of the SR, a loss in optical efficiency occurs. Introduction of a secondary reflector could increase intercept and angular acceptance of the SR system.

6. Outlook

Solar gain simulations aid the industry in making decisions to invest in new solar driven processes and solar process heat installations. As the interest in solar process heat grows, information concerning the expected solar gain from the spectrum of concentrating solar collector systems on the market must be available and expressed in comparable terms.

The model presented in this paper allows the simulation of yearly optical solar gain for future installed systems considering a number of factors previously not accounted for. In combination with thermal models of receivers which will be implemented in future work, prediction of annual solar energy gains will be possible.

There is a margin of error with which the SR approximates its supposed shape for a specific solar declination. As a next step in refinement of the optical model , this shape error needs to be determined and may be described e.g. in terms of a mean angle of deviation either through a finite element analysis or measurement in dependence of the reflector declination.

7. References

Branke, Raymond. 2010. Erstellung eines Modells zur optischen Auslegung von Heliostatenfeldern für solarthermische Turmkraftwerk. Diplomarbeit, Brandenburgische Technische Universität, November 19.

Duffie, John A., and William A. Beckman. 2006. *Solar Engineering of Thermal Processes*. 3rd ed. Hoboken: John Wiley & Sons, Inc.

GTZ. 1997. Installation and testing of a solar steam generator for cooking in India.

Hafner, Bernd. 1999. *Modellierung und Optimierung eines solar betriebenen Prozeßwärmesystems*. 1st ed. Aachen: Shaker Verlag.

Jayasimha, B.K. 2006. Application of Scheflfler Reflectors for Process Industry.

Mertins, Max. 2009. Technische und wirtschaftliche Analyse vonhorizontalen Fresnel-Kollektoren. Universität Karlsruhe (TH).

Neumann, Andreas, Andreas Witzke, Scott A. Jones, and Gregor Schmitt. 2002. "Representative Terrestrial Solar Brightness Profiles." *Journal of Solar Energy Engineering* 124 (2): 198. doi:10.1115/1.1464880.

Oelher, U, and W Scheffler. 1994. "The use of indigenous materials for solar conversion." *Solar Energy Materials and Solar Cells* 33 (3) (July): 379-387. doi:10.1016/0927-0248(94)90239-9.

Pilz, Joachim. 2006. Development and Testing of a 16 m^2 parabolic dish with Cavity Receiver for a Solar Steam System. World Renewal Spiritual Trust (WRST).

Scheffler, Wolfgang, 2010, Personal communication

Hoedt, Heike, 2010, Personal communication

8. Symbols

α	Absorbtance
Ap_0	Area enclosed by the elliptical frame of the Scheffler Reflector at equinox
DNI	Direct normal irradiation
CSR	Circumsolar ratio
δ_r	Declination of the Scheffler Reflector
δ_s	Declination of the sun
η_{opt}	Optical efficiency
I_{bn}	Beam normal irradiation
$\gamma(\mathrm{r})$	Receiver intercept factor
ρ	Reflectance
ρ_{packing}	Packing ratio
SR	Scheffler Reflector
$\sigma_{\mathrm{surface}}$	Specular surface error
σ_{shape}	Shape error
θ	Incidence angle of I_{bn} on the aperture of the Scheffler Reflector
$\theta_{\mathrm{c},\omega}$	Acceptance hour angle
$\theta_{\mathrm{c},\delta}$	Acceptance declination angle